

## Modeling the fuel consumption by a HEV vehicle – a case study

### ARTICLE INFO

Received: 13 October 2022  
Revised: 23 November 2022  
Accepted: 4 December 2022  
Available online: 26 December 2022

*The article presents a mathematical model demonstrating the synergy of HEV energetic machines in accordance with the model predictive control. Then the results of road tests are presented. They were based on the factory control of the above-mentioned system. The results of the operating parameters of the system according to the factory control and the results of the operating parameters according to the model predictive control were compared. On their basis, it could be concluded that the model predictive control contributed to changes in the power and electrochemical charge level of the energy storage system from 50.1% (the beginning) to 56.1% (the end of course) and for MPC from 50.1% (the beginning) to 59.9% (the end of the course). The applied MPC with 13 reference trajectories (LQT) of power machines of the series-parallel HEV allowed for fuel savings on the level of 4%.*

**Key words:** hybrid electric vehicle, fuel consumption, model predictive control, factory control, energy consumption

This is an open access article under the CC BY license (<http://creativecommons.org/licenses/by/4.0/>)

### 1. Introduction

The fuel consumption of HEVs is an important parameter depending on the method of controlling the internal combustion engine, generator and the electric motor. The main purpose of this control is to increase the energy efficiency of the HEV drive system. This control can be defined as the cooperation of assemblies/components remaining in continuous interaction with each other. This can also be considered as energetic machines energy management system [3, 10, 24].

The origins of HEV energy management systems are seen in a control method based on heuristic hypotheses. They assumed the expected operating conditions of the drive system – commencement of operation and its continuation in electrical mode to the set speed or reaching the maximum torque. Within the range that the torque of the electric motor decreased, the drive was supported by an internal combustion engine [14, 17].

Another solution of the energy management system was the use of statistical optimisation. This method did not require knowledge of the actual power demand, but was based only on taking into account its average value [3].

The low accuracy of the mentioned method resulted in the development of the HEV drive energy management system based on stochastic-dynamic programming (DP) [2, 10, 18, 19, 36]. In the model of the hybrid powertrain energy management system, the power demand, determined by the driver, was of a stochastic process characteristics. In the concept, however, the model of a hybrid vehicle was determined. The optimisation of the target function was based on the power demand in general road conditions and not on a specific driving cycle. This resulted in low accuracy of the method [19].

An interesting approach to the issue of energy management of HEVs can be found in [24, 25]. They contain algorithms of the equivalent fuel consumption strategy (ECMS), among others, in HEVs equipped with fuel cells.

Such a control strategy presented as a function of cost (the sum of fuel consumption and energy consumption of a hybrid vehicle) also appears in [11, 30]. The main disadvantage of this type of control is the use of information *a priori* regarding road conditions or conditions for conducting laboratory tests (according to the adopted driving cycle).

Modification of fuel consumption optimisation algorithms (ECMS) for series-parallel electric hybrid vehicles was undertaken by Liu and Peng [19]. The experimental tests carried out by them using the SDP and ECMS strategies resulted in an improvement in the dynamic properties of HEV. They also contributed to the reduction of fuel consumption of the HEV. The energy model of the HEV vehicle powertrain system created by them automatically generated dynamic equations of the system. The demonstrated algorithms implemented an effective synergy of the internal combustion engine with electric machines ensuring a reduction in fuel consumption [20].

Another solution assumed the use of PSO (*particle swarm optimisation*) [1, 6–8, 15, 31]. It was used in a hybrid vehicle enabling charging the traction battery from a power socket (plug-in HEV) [6, 30]. This energy management strategy was based on a real-time algorithm used to reduce fuel consumption. The result of Hwang and Chen's research was an improvement in fuel consumption to 9.4% compared to the base control model [15].

In parallel, research was conducted on the model predictive control in energy management in HEVs [16]. The control applied enabled optimal torque distribution for the parallel hybrid powertrain of the vehicle. The cost function used in the strategy was minimised thanks to telemetric estimation of vehicle speed [16].

Research was also carried out using model predictive control in parallel-series HEVs equipped with a supercapacitor [5].

Simultaneously, experiments were carried out with HEVs equipped with a series powertrain system. A strategy

to minimise fuel consumption was developed thanks to the use of stochastic optimisation of the management process using the Markov chain [23].

Model predictive control was also used to determine exits from the system (economical driving reducing fuel consumption) and also relied on information provided by the Intelligent Transport System [36].

This energy management system was developed in [34, 35]. Linear square tracking (LQT) was applied to the model predictive control. It supported the effective control of power distribution in a series-parallel HEV. At the same time, the LQT controller minimised the cost function, maintaining the level of charge of the energy storage system at the desired level [34, 35].

Another method of exercising model predictive control in the energetic machines energy management model of a HEV was also invented. Non-linear predictive control (NMPC) has saved up to 8.8% of fuel consumption according to the NEDC cycle. This result was obtained by comparing the values to the Factory Vehicle Energy Management System [31].

The energy model of a series-parallel HEV is also presented in the article [6]. It was characterised by high accuracy; however, it was based on NEDC and HWYCOL road tests.

It is also important to mention about the other actual effective energy management systems proposed in HEVs. It was based on distributed deep reinforcement learning (DRL). Paper presented DRL algorithms just like: a deep q-network (DQN), asynchronous advantage actor-critic (A3C) and distributed proximal policy optimization (DPPO). Simulation results show that tree DRL based control strategies can achieve near optimal fuel economy but also outstanding computational efficiency [32].

It is worth noting that above all presented energy management systems, the MPC is a proven and effective method used by many researchers [28, 34–36]. But the main problem of MPC is that it is useless to achieve a lower level of HEV fuel consumption without reference trajectory (infinite prediction horizon). So, as it was mentioned, LQT with MPC can reduce fuel consumption [34, 35]. But it was proven only for maximum load of ICE. It was only one reference trajectory. An important aspect is how to reach the lower level of HEV fuel consumption? Maybe the use of dozen reference trajectories, not only for maximum power but also for partial loads of ICE, would solve this problem? To reach this, it is required to collect operational points of ICE under real conditions. Only a few works were carried out in road conditions, e.g. [4, 27–29] not based on simulations or observations and measurements in stationary (laboratory) conditions [15, 30, 32–35].

In real life operation, it is possible to get more necessary information useful to optimise the HEV energy management control. This translates into its mileage of fuel consumption.

The vast majority of the publications cited outline the study of the mileage fuel consumption of the HEV in stationary conditions. The experiments are then carried out on the basis of specific road tests (often poorly reflecting the actual road conditions). However, there is no information

on changes in the mileage fuel economy of the HEV in actual road operation using the model predictive control mode. Hence, it seemed necessary to carry out tests of the mileage fuel consumption value of the HEV vehicle with the model predictive control. For this purpose, a diagnostic computer for a specific car model was used. Such research is a novelty in this field. The above observations became the basis for formulating the main purpose of the work.

## 2. Purpose and scope of research

The aim of the study was to assess the fuel consumption of HEV with model predictive control in real road conditions (case study).

Raising this issue was due to the insufficient level of knowledge about the impact of the change in the energetic machines management control in the HEV concerned on its fuel consumption (in real road conditions). The additional purpose of the research was to verify the energetic machines operating parameters of the series-parallel HEV powertrain system.

The basic study questions were as follows: 1) does MPC strategy with 13 reference trajectories really contribute to improving the fuel economy of a HEV? 2) does this EMS have a good effect on the battery state of charge (SOC)?

The aim of the work is considered to be achieved when the answers to the research questions are obtained. The values of operational parameters during real vehicle traffic conditions should be taken as the basic evaluation criterion. Within the framework of the defined objective of the work the following specific objectives were implemented: – determination of percentage differences in the course of fuel consumption according to MPC with 13 reference trajectories (LQT) and factory control, – comparison of the obtained values with the values provided by the vehicle manufacturer. Experimental assessment of HEV fuel consumption in real road conditions as the main scientific goal will allow to prove the rightness and to indicate the benefits of the MPC with 13 reference trajectories application of the HEV working machines.

The scope of research will be based on the experimental method. It will include tests of the fuel consumption of the HEV with factory control in real road conditions. Then, the values of the parameters of the internal combustion engine and electrical machines will be simulated. This will be implemented in accordance with the energy management strategy for model predictive control – also in real road conditions.

The studies will be carried out in urban and extra-urban traffic conditions with the use of a specific HEV vehicle. They will be carried out in accordance with the presented HEV energy consumption model.

The subject of the studies will be a Toyota Prius 3 car (produced in 2012), a HEV equipped with a series-parallel hybrid powertrain system.

The technical and operational characteristics of the test object are presented in Table 1 [13, 19].

## 3. HEV energy consumption model

In order to determine the value of the mileage fuel consumption of the HEV according to the predictive control, it was necessary to determine the type of parameters related to the cost function. These included:

- power of the internal combustion engine,
- angular speed of the internal combustion engine,
- power of the generator,
- angular speed of the generator,
- power of the electric motor,
- the angular speed of the electric motor,
- power of the traction battery,
- the level of charge of the traction battery.

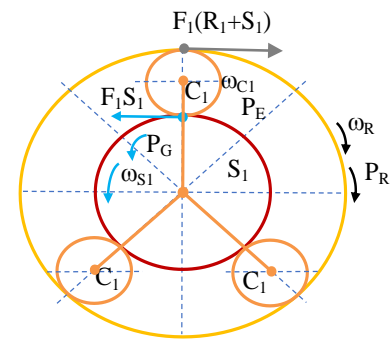
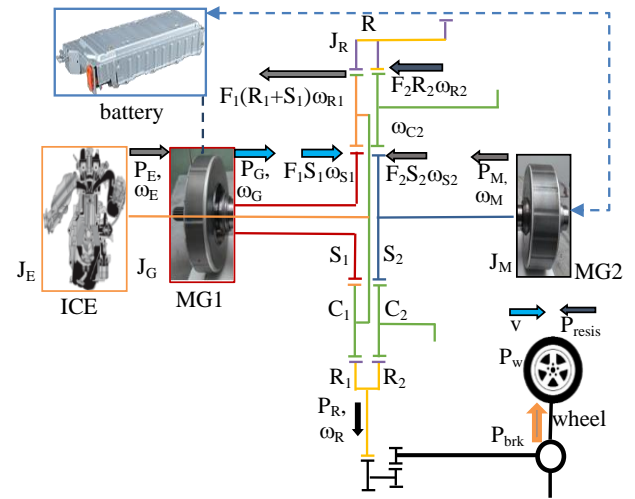
The indicated parameters are related to the power transmission in the powertrain system of the HEV.

Table 1. Specifications of Toyota Prius 3 2012 vehicle [13]

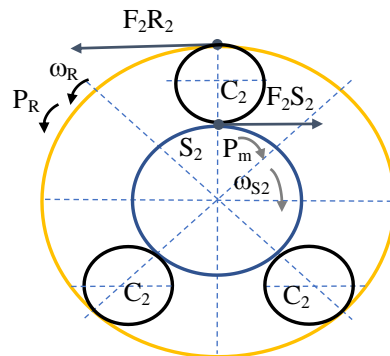
Parameter	Unit	Value
Total mass	kg	1630
Wheel dynamic radius	m	0.29
Wheels moment of inertia	kg m <sup>2</sup>	2.7
Facing Surface	m <sup>2</sup>	1.62
Rolling resistance coefficient	–	0.0084
Air drag coefficient	–	0.25
Drive system type	–	Series and parallel
Internal combustion engine		
Ignition type		spark ignition
Capacity	dm <sup>3</sup>	1.8
Number of cylinders		4
Max. power	kW	73
Max. power rotational speed	rpm	5200
Max. torque	Nm	142
Max. torque rotational speed	rpm	4000
Mass moment of inertia	kg m <sup>2</sup>	0.18
Generator (MG1)		
Type	–	three-phase synchronous AC
Function	–	generator, ICE starter
Rated voltage	V	650
Maximum output power	kW	42
Max torque	Nm	45
Current at max torque	A	75
Max. rotational speed	rpm	10,000
Mass moment of inertia	kg m <sup>2</sup>	0.023
Electric motor (MG2)		
Type		three-phase synchronous AC
Function		generator, wheel drive
Rated voltage	V	650
Maximum output power	kW	60
Maximum torque	Nm	207
Current at max torque	A	230
Max. rotational speed	rpm	13000
Mass moment of inertia	kg m <sup>2</sup>	0.05
Electrochemical accumulation system and inverter		
Battery type		NiMH
Nom. voltage	V	201.6
Capacity	Ah	6.5

### 3.1. Power transmission in the powertrain system

The power generated by the internal combustion engine is transferred to the yoke of the satellite wheels. Then it is directed onto the planetary gear crown wheel. After exiting the planetary gearbox, the power drives the axles of the vehicle's wheels using the counter drive gear and the final drive gear. The MG1 generator, connected to the sun gear, acts as a starter and is used to charge the battery while driving. The MG2 electric machine is connected to the sun gear of the second planetary gear. It is designed to support the internal combustion engine in generating power, but also to ensure energy recovery during braking [22] (Fig. 1).



a) first planetary gear (ICE side)



b) second planetary gear (MG2 side)

Fig. 1. Power transfer dynamics in the series-parallel powertrain system of the HEV

The operation of the above system is described by the following angular speed relationships [22]:

$$\omega_{C1} = \frac{R_1}{S_1 + R_1} \omega_R + \frac{S_1}{S_1 + R_1} \omega_{S1} \quad (1)$$

$$\omega_{C2} = \frac{R_2}{S_2 + R_2} \omega_R + \frac{S_2}{S_2 + R_2} \omega_{S2} \quad (2)$$

The yoke of the second gear's satellites is blocked, therefore  $\omega_{C2} = 0$ .

$$0 = \frac{R_2}{S_2 + R_2} \omega_R + \frac{S_2}{S_2 + R_2} \omega_{S2} \quad (3)$$

$$\frac{R_2}{S_2 + R_2} \omega_R = -\frac{S_2}{S_2 + R_2} \omega_{S2} \quad (4)$$

$$\omega_R = -\frac{S_2}{R_2} \omega_{S2} \quad (5)$$

$$\omega_{S2} = \omega_M, \omega_{C1} = \omega_E, \omega_{S1} = \omega_G \quad (6)$$

$$\omega_R = -\frac{S_2}{R_2} \omega_M \quad (7)$$

$$\omega_E = \frac{R_1}{S_1 + R_1} \omega_R + \frac{S_1}{S_1 + R_1} \omega_G \quad (8)$$

$$\omega_E = -\frac{R_1}{S_1 + R_1} \cdot \frac{S_2}{R_2} \omega_M + \frac{S_1}{S_1 + R_1} \omega_G \quad (9)$$

$$\omega_M = -\frac{R_2}{S_2} \omega_R \quad (10)$$

$$\omega_G = \frac{\omega_E(R_1 + S_1)}{S_1} + \frac{R_1}{S_1} \frac{S_2}{R_2} \cdot \omega_M \quad (11)$$

As it can be seen from the above relationships, the angular speeds of individual HEV energy machines are closely related.

The angular speed at the output of the gearbox results from the angular speeds of individual energetic machines. The vehicle speed is described by the following relationship [35]:

$$v = \frac{\omega_R \cdot r_d}{i_{FD}} \quad (12)$$

Limitations of power transmission in the powertrain system:

a) power of the internal combustion engine:

$$0 \leq P_E \leq P_E^{\max} \quad (13)$$

b) angular speed of the internal combustion engine:

$$\omega_E^{\min} \leq \omega_E \leq \omega_E^{\max} \quad (14)$$

c) power of the generator (MG1):

$$P_G^{\min} \leq P_G \leq P_G^{\max} \quad (15)$$

d) angular speed of the generator (MG1):

$$\omega_G^{\min} \leq \omega_G \leq \omega_G^{\max} \quad (16)$$

(e) power of the electric motor (MG2):

$$P_M^{\min} \leq P_M \leq P_M^{\max} \quad (17)$$

(f) rotational speed of the electric motor (MG2):

$$\omega_M^{\min} \leq \omega_M \leq \omega_M^{\max} \quad (18)$$

The propulsion system of the HEV is characterised by different relationships when the vehicle is in the steady conditions or unsteady conditions.

### 3.2. Movement of the HEV under steady state conditions

During the steady movement of the vehicle, there is no resistance to inertia forces, hence the mass moments of inertia of individual energetic machines are not taken into account. Then the operation of the powertrain system (Fig. 1) describe the following equations [26, 32]:

$$P_E \cdot \eta_{C1/R} \cdot \omega_E^{-1} = F_1(R_1 + S_1) \quad (19)$$

$$P_G \cdot \eta_{S1/C1} \cdot \omega_G^{-1} = -F_1 S_1 \quad (20)$$

$$P_M \cdot \eta_{R2/R} \cdot \omega_M^{-1} = F_2 S_2 \quad (21)$$

It can also be noted that the output power of the system depends on the power of individual power machines:

$$P_E \cdot \eta_{C1/R} + P_M \cdot \eta_{R2/R} = P_R \quad (22)$$

Hence, the power acting on the wheels of the vehicle, taking into account the output power of the system and the efficiency of the main transmission, takes the form of:

$$P_W = P_R \cdot \eta_{fd} = (P_E \cdot \eta_{C1/R} + P_M \cdot \eta_{R2/R}) \cdot \eta_{fd} \quad (23)$$

The movement of the HEV under steady state conditions is characterised by a constant speed. In such conditions, when driving on a smooth, straight road (without bends), the HEV overcomes rolling resistance, air resistance, or hill resistance. Then, the relation of the HEV movement, expressed by the power acting on the wheels, is as follows:

$$P_W = F_p \cdot v \quad (24)$$

$$P_W = P_{resis} \quad (25)$$

$$P_W = F_{resis} \cdot v = (F_r + F_s + F_a) \cdot v \quad (26)$$

$$P_W = (mgf_r \cos \alpha + mg \sin \alpha + \frac{1}{2} \rho_A \cdot C_d A_f v^2) \cdot v \quad (27)$$

### 3.3. Vehicle movement under unsteady (transient) state conditions

During the transient movement of the vehicle there are inertia resistances, hence in this case the mass moments of inertia of individual energetic machines are taken into account. This is described in the following equations [28, 34]:

$$J_E \cdot \dot{\omega}_E = P_E \cdot \eta_{C1/R} \omega_E^{-1} - F_1(R_1 + S_1) \quad (28)$$

$$J_G \cdot \dot{\omega}_G = P_G \cdot \eta_{S1/C1} \cdot \omega_G^{-1} + F_1 S_1 \quad (29)$$

$$J_M \cdot \dot{\omega}_M = P_M \cdot \eta_{R2/R} \cdot \omega_M^{-1} - F_2 S_2 \quad (30)$$

$$\begin{aligned} J_R \cdot \dot{\omega}_R &= F_1 R_1 + F_2 R_2 - P_R \omega_R^{-1} \\ &= \frac{R_1}{R_1 + S_1} P_E \cdot \eta_{C1/R} \omega_E^{-1} + \frac{R_2}{S_2} \cdot P_M \\ &\quad \cdot \eta_{R2/R} \cdot \omega_M^{-1} - P_R \omega_R^{-1} \end{aligned} \quad (31)$$

The movement of the HEV in transient conditions is characterised by variable speed. In such conditions, when

driving on a smooth, straight road (without bends), the HEV overcomes rolling resistance, air resistance, inertia resistance, or potentially hill resistance. Then the relation of the movement of the HEV, expressed through the power on the wheels, takes the form of:

$$P_w = \int_{v_1}^{v_2} F_{\text{resis}} dv = \int_{v_1}^{v_2} (F_r + F_s + F_i + F_a) dv \quad (32)$$

$$P_w = \int_{v_1}^{v_2} (mgf_r \cos \alpha + mg \sin \alpha + \delta \cdot m \cdot a + \frac{1}{2} \rho_A \cdot C_d A_f v^2) dv \quad (33)$$

When overcoming inertia resistance by the vehicle, an important parameter is the rotating mass coefficient. Taking into account the mass moments of inertia of energetic machines, it takes the following form:

$$\delta = w_1 + w_2 \cdot i_G^2 + w_3 \cdot i_E^2 + w_4 \cdot i_M^2 \quad (34)$$

$$w_1 = 1 + \frac{g}{G} \cdot \frac{J_k}{r_d^2} \quad (35)$$

$$w_2 = \frac{g}{G} \cdot \frac{J_G \cdot \eta_{fd} \cdot i_{fd}^2}{r_d^2} \quad (36)$$

$$w_3 = \frac{g}{G} \cdot \frac{J_E \cdot \eta_{fd} \cdot i_{fd}^2}{r_d^2} \quad (37)$$

$$w_4 = \frac{g}{G} \cdot \frac{J_M \cdot \eta_{fd} \cdot i_{fd}^2}{r_d^2} \quad (38)$$

Using relations from (28) to (31) with the assumptions of the model ( $J_R \approx 0$ ), a simplified version of the predictive control model is presented below:

$$\left[ J_E + J_G \left( \frac{R_1 + S_1}{S_1} \right)^2 \right] \cdot \dot{\omega}_E - \left[ J_G \frac{R_1 \cdot S_2 \cdot (R_1 + S_1)}{R_2 \cdot S_1^2} \right] \cdot \dot{\omega}_M = P_E \cdot \eta_{C_1/R} \cdot \omega_E^{-1} + P_G \cdot \frac{(R_1 + S_1)}{S_1} \cdot \eta_{S_1/C_1} \cdot \omega_G^{-1} \quad (39)$$

$$\begin{aligned} & \left[ J_E \cdot \frac{R_1}{R_1 + S_1} \right] \dot{\omega}_E + \left[ J_M \frac{R_2}{S_2} - m \cdot \left( \frac{r_d}{f_d} \right)^2 \cdot \frac{S_2}{R_2} \right] \cdot \dot{\omega}_M \\ & = P_E \cdot \frac{R_1}{R_1 + S_1} \eta_{C_1/R} \cdot \omega_E^{-1} + P_M \cdot \frac{R_2}{S_2} \eta_{R_2/R} \\ & \cdot \omega_M^{-1} + \frac{T_{brk} \cdot \eta_{fd}}{f_d} + \frac{1}{2} \cdot \rho_A \cdot C_d \cdot A_f \\ & \cdot \frac{S_2^2 \cdot \omega_M^2 \cdot r_d^3}{R_2^2 \cdot f_d^3} - mg \cdot \frac{r_d}{f_d} (f_r \cos \alpha + \sin \alpha) \end{aligned} \quad (40)$$

### 3.4. Operation of the electrochemical energy storage system

The full electric hybrid powertrain system of the vehicle assumes the efficient use of an electric power source. The status of available electricity is reflected in the battery charge level (SOC) [12, 20, 34, 35]:

$$SOC = \frac{Q_{\text{max}} - Q_{\text{used}}}{Q_{\text{max}}} \cdot 100\% \quad (41)$$

The used electrical capacity of the battery is described by the following relation:

$$Q_{\text{used}} = \begin{cases} \int_0^t I_{\text{bat}} \cdot dt \\ \int_0^t I_{\text{bat}} \eta_{\text{coulomb}} dt \end{cases} \quad (42)$$

Please note that  $I_{\text{bat}} > 0$  (discharging),  $I_{\text{bat}} < 0$  (charging). Hence, the derivative of the electrochemical charge level of the energy storage system can be presented as follows:

$$\dot{SOC} = - \frac{I_{\text{bat}}}{Q_{\text{max}}} \quad (43)$$

Power of the electrochemical energy storage system:

$$\begin{aligned} P_{\text{bat}} &= U_{\text{bus}} \cdot I_{\text{bat}} = (V_{\text{oc}} - I_{\text{bat}} \cdot r_{\text{bat}}) \cdot I_{\text{bat}} \\ &= V_{\text{oc}} I_{\text{bat}} - I_{\text{bat}}^2 \cdot r_{\text{bat}} \end{aligned} \quad (44)$$

Ultimately, the charging or discharging current of the battery takes the following form:

$$\dot{SOC} = - \frac{V_{\text{oc}} - \sqrt{V_{\text{oc}}^2 - 4r_{\text{bat}} P_{\text{bat}}}}{2r_{\text{bat}} Q_{\text{max}}} \quad (45)$$

The power of the energy storage system  $P_{\text{bat}}$  is used during all driving modes. Both during the drive or recuperation process. To cover the power demand generated by the generator and/or the electric motor according to the following relation:

$$P_{\text{bat}} = P_G \cdot \eta_G^k \cdot \eta_{C_1}^k + P_M \cdot \eta_M^k \cdot \eta_{C_2}^k = P_{\text{des}} - P_E \quad (46)$$

$P_{\text{des}}$  is the power expected through pressing the accelerator or brake pedal. The power of the energy storage system shall be either a positive value during discharge or a negative value during charging.

### 3.5. Restrictions to the energy storage system

The applied energy management strategy – the predictive control is characterised by specific limitations of the energy storage system:

a) traction battery power:

$$P_{\text{bat}}^{\text{min}} \leq P_{\text{bat}} \leq P_{\text{bat}}^{\text{max}} \quad (47)$$

(b) the level of charge of the traction battery:

$$SOC^{\text{min}} \leq SOC \leq SOC^{\text{max}} \quad (48)$$

The mathematical model has been linearised to the specific conditions. The linear form of the MPC model is represented by the matrices:

$$\begin{aligned} & \begin{bmatrix} E_{11} & -E_{12} \\ E_{21} & E_{22} - \rho_A \cdot C_d \cdot A_f \cdot \frac{S_2^2 \cdot r_d^3}{R_2^2 \cdot f_d^3} \end{bmatrix} \cdot \begin{bmatrix} \dot{\omega}_E \\ \dot{\omega}_M \end{bmatrix} \\ & = \begin{bmatrix} \eta_{C_1/R} \cdot \omega_E^{-1} & \frac{R_1}{R_1 + S_1} \cdot \eta_{S_1/C_1} & 0 \\ \frac{R_1}{R_1 + S_1} \eta_{C_1/R} & 0 & \frac{R_2}{S_2} \eta_{R_2/R} \end{bmatrix} \begin{bmatrix} P_E \cdot \omega_E^{-1} \\ P_G \cdot \omega_G^{-1} \\ P_M \cdot \omega_M^{-1} \end{bmatrix} \end{aligned} \quad (49)$$

where:

$$\begin{aligned} E_{11} &= J_E + J_G \left( \frac{R_1 + S_1}{S_1} \right)^2, \quad E_{12} = \left[ J_G \frac{R_1 \cdot S_2 \cdot (R_1 + S_1)}{R_2 \cdot S_1^2} \right], \\ E_{21} &= \left[ J_E \cdot \frac{R_1}{R_1 + S_1} \right], \quad E_{22} = \left[ J_M \frac{R_2}{S_2} - m \cdot \left( \frac{r_d}{f_d} \right)^2 \cdot \frac{S_2}{R_2} \right] \\ E_D &= E_{11} (E_{22} - \rho \cdot C_d \cdot A_f \cdot \frac{S_2^2 \cdot r_d^3}{R_2^2 \cdot f_d^3}) + E_{12} \cdot E_{21} \end{aligned} \quad (50)$$

### 3.6. Mileage fuel consumption

The mileage fuel consumption of the HEV is a result of several other parameters. Not only the fuel consumption of the internal combustion engine, but also the equivalent fuel consumption of the electric motor should be taken into account here. This is described in the following relations showing the relationships between the required power values of the internal combustion engine and the electric motor [28, 35]:

$$b = \frac{\dot{m}}{P_E} \quad (51)$$

$$\dot{m} = b \cdot P_E = \frac{P_{E_{des}}}{\eta_E \cdot W_u} \quad (52)$$

The calorific value of the fuel (petrol) was equal to  $44 \cdot 10^6$  J/kg. The equivalent fuel consumption, calculated on the basis of the consumed energy of the traction battery, has been determined in accordance with the formula:

$$\dot{m}_{eq} = C_{bat} \cdot P_{bat} = C_{bat} \cdot V_{oc} \cdot I_{bat} \quad (53)$$

Ultimately, the equivalent fuel consumption takes the form of:

$$\dot{m}_{eq} = \frac{C_{bat}}{2r_{bat}} [V_{oc}^2 - V_{oc} \cdot \sqrt{V_{oc}^2 - 4r_{bat}P_{bat}}] \quad (54)$$

The value of the equivalent fuel consumption coefficient  $C_{bat}$  was determined and equalled 0.0000227. The parameter was determined on the basis of the equivalent fuel consumption. As the power of the traction battery to the calorific value of the fuel coefficient. According to [11], the values of  $b_1$  and the coefficient  $a_1$  were adopted from 0.0000227 to 0.0000237.

Taking into account the above relationships, the instantaneous fuel consumption of the HEV (related to the distance) can be described using the formula:

$$Q = \frac{100 \cdot (\dot{m} + \dot{m}_{eq})}{3600 \cdot \rho_F \cdot v} = \frac{\dot{m} + \dot{m}_{eq}}{36 \cdot \rho_F \cdot v} \quad (55)$$

The mileage consumption of the HEV is related to the cost function, which is associated with the predictive control model of the HEV's powertrain system energetic machines. The main objective of the presented energy management system is to minimise fuel consumption and equivalent fuel consumption. The parameter describing the total fuel consumption of the vehicle is determined by the relation [16]:

$$J = \sum_{s=0}^{N-1} (\text{fuel}_s + \alpha_E \Delta_{SOC}^2) \rightarrow \min \quad (56)$$

$$\Delta_{SOC} = \begin{cases} SOC_s - SOC_d & SOC_s < SOC_d \\ 0 & SOC_k \geq SOC_d \end{cases} \quad (57)$$

Using the previous dependencies, the cost function takes the following form:

$$J = \int_0^{N \cdot t_d} \rho \left( \left[ \dot{m}(P_{E_{des}}, \tau) \right]^2 + \left[ \dot{m}_{eq}(P_{G_{des}}, P_{M_{des}}, \tau) \right]^2 \right) d\tau \rightarrow \min \quad (58)$$

The expected value of the torque in the function of cost is related to the value of the output power from the system. Relation (58) takes the form of [34, 37]:

$$J = \int_0^{N \cdot t_d} [P_{pre}(\tau) - P_R]^2 + \rho \left( \left[ \dot{m}(P_{E_{des}}, \tau) \right]^2 + \left[ \dot{m}_{eq}(P_{G_{des}}, P_{M_{des}}, \tau) \right]^2 \right) d\tau \rightarrow \min \quad (59)$$

Since the function of cost is non-linear, according to relation (59) the control of the output parameters must be converted to the category  $m$  and  $m_{eq}$ :

$$P_{E_{des}} = \eta_E \cdot W_u \cdot \dot{m} \quad (60)$$

Equations (51) and (53) take the form:

$$P_{des} = \frac{\dot{m}_{eq}}{C_{bat}} - \frac{r_{bat} \cdot \dot{m}_{eq}^2}{V_{oc}^2 \cdot C_{bat}} + P_E \quad (61)$$

The linear model of the operational points themselves is as follows:

$$\dot{T}_E = -\frac{1}{\tau_E} T_E + \Gamma_{e\omega_e} \cdot \omega_E + \Gamma_{em} \cdot \dot{m} \quad (62)$$

$$\dot{T}_G = \Gamma_{GTE} \cdot T_E - \frac{1}{\tau_G} T_G \quad (63)$$

$$\begin{aligned} \dot{T}_M = & \Gamma_{MTE} \cdot T_E - \frac{1}{\tau_M} T_M + \Gamma_{M\omega_E} \cdot \omega_E + \Gamma_{M\omega_M} \cdot \omega_M \\ & + \Gamma_{Meq} \cdot \dot{m}_{eq} \end{aligned} \quad (64)$$

where:

$$\Gamma_{e\omega_e} = -\frac{1}{\tau_E} \cdot \frac{\eta_e \cdot W_u \cdot \dot{m}_0}{\omega_{E0}^2}, \Gamma_{em} = \frac{1}{\tau_E} \cdot \frac{\eta_e \cdot W_u}{\omega_{E0}} \quad (65)$$

$$\Gamma_{GTE} = -\frac{1}{\tau_G} \cdot \frac{S_1}{R_1 + S_1} \quad (66)$$

$$\Gamma_{MTE} = -\frac{1}{\tau_M} \cdot \left( \frac{R_1}{S_1 + R_1} \cdot \frac{S_2}{R_2} - \frac{\omega_{E0}}{\omega_{M0}} \right) \quad (67)$$

$$\Gamma_{M\omega_E} = \frac{1}{\tau_M} \cdot \frac{T_{E0}}{\omega_{M0}} \quad (68)$$

$$\Gamma_{M\omega_M} = -\frac{1}{\tau_M \cdot \omega_{M0}^2} \cdot \left( \frac{\dot{m}_{eq0}}{C_{bat}} - \frac{r_{bat} \cdot \dot{m}_{eq0}^2}{V_{oc}^2 \cdot C_{bat}^2} + T_{E0} \cdot \omega_{E0} \right) \quad (69)$$

$$\Gamma_{Meq} = -\frac{1}{\tau_M \cdot C_{bat} \cdot \omega_{M0}} \cdot \left( 1 - 2 \frac{r_{bat}}{V_{oc}^2 \cdot C_{bat}} \right) \quad (70)$$

The linear form of the energy management model is as follows:

$$\begin{cases} \dot{x} = A_c x + B_c u \\ y = C_c x + D_c u \end{cases}, u = \begin{bmatrix} \dot{m} \\ \dot{m}_{eq} \end{bmatrix}, y = P_R \quad (71)$$

Equation describing  $A_c$ :

$$\mathbf{A}_c = \begin{bmatrix} 0 & -\frac{1}{\tau_E} & 0 & 0 & \Gamma_{e\omega e} & 0 & 0 \\ \Gamma_{GTE} & 0 & -\frac{1}{\tau_G} & 0 & 0 & 0 & 0 \\ \Gamma_{MTE} & 0 & 0 & -\frac{1}{\tau_M} & \Gamma_{M\omega E} & \Gamma_{M\omega M} & 0 \\ \frac{E_{22}}{E_D} - \rho \cdot C_d \cdot A_f \cdot \frac{S_2^2 \cdot r_d^3}{R_2^2 \cdot f_d^3 \cdot E_D} + \frac{E_{12}}{E_D} \left( \frac{R_1}{R_1 + S_1} \right) & \frac{E_{22}}{E_D} - \rho \cdot C_d \cdot A_f \cdot \frac{S_2^2 \cdot r_d^3}{R_2^2 \cdot f_d^3 \cdot E_D} \left( \frac{R_1}{R_1 + S_1} \right) & \frac{E_{12}}{E_D} \frac{R_2}{S_2} & 0 & 0 & 0 & 0 \\ -\frac{E_{21}}{E_D} + \frac{E_{11}}{E_D} \left( \frac{R_1}{R_1 + S_1} \right) & -\frac{E_{21}}{E_D} \left( \frac{R_1}{R_1 + S_1} \right) & \frac{E_{11} \cdot R_2}{E_D \cdot S_2} & 0 & 0 & 0 & 0 \\ 0 & \Gamma_{sG} & \Gamma_{sM} & \Gamma_{s\omega e} & \Gamma_{s\omega M} & 0 & 0 \end{bmatrix} \quad (72)$$

$$\mathbf{x} = \begin{bmatrix} P_E \\ P_G \\ P_M \\ \omega_E \\ \omega_M \\ SOC \end{bmatrix} \quad (73)$$

$$\mathbf{B}_c = \begin{bmatrix} \Gamma_{em} & 0 \\ 0 & 0 \\ 0 & \Gamma_{Meq} \\ 0 & 0 \\ 0 & 0 \end{bmatrix} \quad (74)$$

$$\mathbf{C}_c^T = \begin{bmatrix} R_1 \\ R_1 + S_1 \\ 0 \\ R_2 \\ S_2 \\ 0 \\ 0 \\ 0 \end{bmatrix} \quad (75)$$

$$\mathbf{D}_c = 0 \quad (76)$$

$$\dot{\mathbf{x}} = \mathbf{A}_c \mathbf{x} + \mathbf{B}_c \mathbf{u} \quad (77)$$

$$\mathbf{y} = \mathbf{C}_c \mathbf{x}$$

where  $\mathbf{A}_c$  described in (72):

The solution of the mathematical model presented above is the use of the LQT controller (Fig. 2) and the conversion of the analytical version of the model to a discrete version.

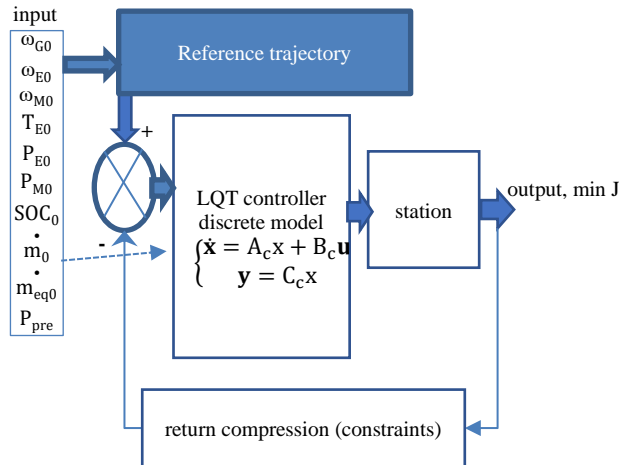


Fig. 2. LQT algorithm architecture

The LQT controller uses input parameters that are the parameters of the model. Also, the linear form of the model (discrete) in order to search for the optimal (minimum) solution of the cost function  $J$ . The return compression is supposed to provide the optimal value of the cost function.

The values of the input parameters for the implementation of the presented LQT algorithm are presented in Table 2.

Table 2. Simulation parameters

Machine	Parameter	Value
Vehicle	total weight	1630 kg
combustion engine	start delay	0.5 s
	time constant	1 s
	max. output power	73 kW
electric motor	output power	60 kW
electrochemical energy storage system	SOC upper level	0.75
	SOC lower level	0.45
	SOC objective	0.60

## 4. Test results

### 4.1. Statistics of ICE

The most important parameter that affects power was the torque of ICE. Within 616 seconds of travel, in the test it was measured 241 ICE operating points. This parameter has been ordered from the minimum to maximum value. After that, the created series was divided into groups. After calculating the frequency of occurrences in a given group, we obtained a distributive series. Each distributive series was characterized by the class intervals of groups and the number of cases occurring in subsequent groups. These are the parameters of the ICE statistics (Table 3) that were used to describe the distributive series.

Table 3. ICE statistics parameters

Distributive series – torque of the ICE	
Parameter	Value
Number of observations (n)	241
Number of classes (k)	$\sqrt{241} = 15.52 \sim 16$
Minimum value (Min)	0.01 Nm
Maximum value (Max)	142 Nm
Max-min	141.99 Nm
(Max-min)/k	8.87~9
Descriptive statistics – torque of the ICE	
Average	23.36 Nm
Median	12.23 Nm
Variance	670.93 Nm
Standard deviation	25.90 Nm
Lower Quartile	2.78 Nm
Upper Quartile	36.83 Nm
Skewness	1.33
Kurtosis	1.14

According to the presented graph (Fig. 2), the values of the ICE torque were divided into 16 classes. But in the last 3 classes (117...142 Nm) there were no torque operating points. For this reason, 13 value classes have been selected to declare 13 reference trajectories.

13 reference trajectories were described in Table 4 (below) and were used in LQT algorithm architecture (Fig. 2).

There were estimated based the equations of trend curves (values of ICE torque).

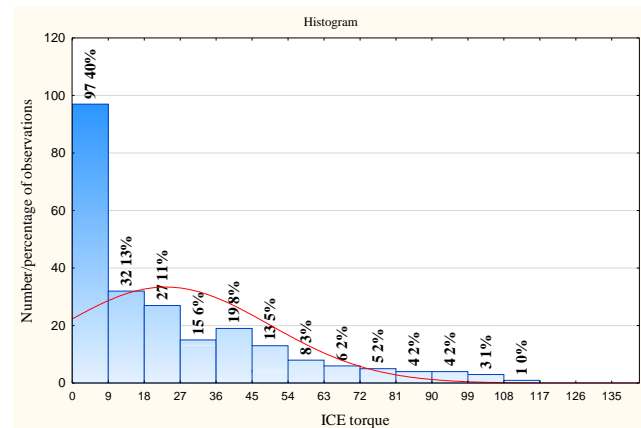


Fig. 2. Histogram of ICE torque (red line – expected normal)

Table 4. Reference trajectory

IF $0 < T_E \leq 9$ Nm THEN:	$T_{Edes} = -7 \cdot 10^{-7} \cdot n_E^2 + 0.0033 \cdot n_E - 0.3969$ $P_{Edes} = T_{Edes} \cdot \omega_E$ $P_{Edes} = P_E$
IF $9 < T_E \leq 18$ Nm THEN:	$T_{Edes} = 3 \cdot 10^{-8} \cdot n_E^2 - 0.0016 \cdot n_E + 14.903$ $P_{Edes} = T_{Edes} \cdot \omega_E$ $P_{Edes} = P_E$
IF $18 < T_E \leq 27$ Nm THEN:	$T_{Edes} = -1 \cdot 10^{-6} \cdot n_E^2 + 0.0053 \cdot n_E + 16.245$ $P_{Edes} = T_{Edes} \cdot \omega_E$ $P_{Edes} = P_E$
IF $27 < T_E \leq 36$ Nm THEN:	$T_{Edes} = -1 \cdot 10^{-6} \cdot n_E^2 - 0.0058 \cdot n_E + 38.056$ $P_{Edes} = T_{Edes} \cdot \omega_E$ $P_{Edes} = P_E$
IF $36 < T_E \leq 45$ Nm THEN:	$T_{Edes} = -1 \cdot 10^{-6} \cdot n_E^2 + 0.001 \cdot n_E + 42.293$ $P_{Edes} = T_{Edes} \cdot \omega_E$ $P_{Edes} = P_E$
IF $45 < T_E \leq 54$ Nm THEN:	$T_{Edes} = 4 \cdot 10^{-7} \cdot n_E^2 - 0.0008 \cdot n_E + 48.387$ $P_{Edes} = T_{Edes} \cdot \omega_E$ $P_{Edes} = P_E$
IF $54 < T_E \leq 63$ Nm THEN:	$T_{Edes} = -6 \cdot 10^{-6} \cdot n_E^2 + 0.0196 \cdot n_E + 46.391$ $P_{Edes} = T_{Edes} \cdot \omega_E$ $P_{Edes} = P_E$
IF $63 < T_E \leq 72$ Nm THEN:	$T_{Edes} = -2 \cdot 10^{-6} \cdot n_E^2 + 0.0069 \cdot n_E + 59.273$ $P_{Edes} = T_{Edes} \cdot \omega_E$ $P_{Edes} = P_E$
IF $72 < T_E \leq 81$ Nm THEN:	$T_{Edes} = -1 \cdot 10^{-5} \cdot n_E^2 + 0.00457 \cdot n_E + 42.177$ $P_{Edes} = T_{Edes} \cdot \omega_E$ $P_{Edes} = P_E$
IF $81 < T_E \leq 90$ Nm THEN:	$T_{Edes} = -3 \cdot 10^{-5} \cdot n_E^2 + 0.0859 \cdot n_E + 27.572$ $P_{Edes} = T_{Edes} \cdot \omega_E$ $P_{Edes} = P_E$
IF $90 < T_E \leq 99$ Nm THEN:	$T_{Edes} = -0.0002 \cdot n_E^2 + 0.3827 \cdot n_E - 130.24$ $P_{Edes} = T_{Edes} \cdot \omega_E$ $P_{Edes} = P_E$
IF $99 < T_E \leq 135$ Nm THEN:	$T_{Edes} = 5 \cdot 10^{-5} \cdot n_E^2 - 0.1633 \cdot n_E + 240.11$ $P_{Edes} = T_{Edes} \cdot \omega_E$ $P_{Edes} = P_E$
IF $135 < T_E \leq 142$ Nm THEN:	$T_{Edes} = -4 \cdot 10^{-6} \cdot n_E^2 + 0.035 \cdot n_E + 73.868$ $P_{Edes} = T_{Edes} \cdot \omega_E$ $P_{Edes} = P_E$

## 4.2. Speed profile

On Figure 3 it was presented speed profile during the road tests.

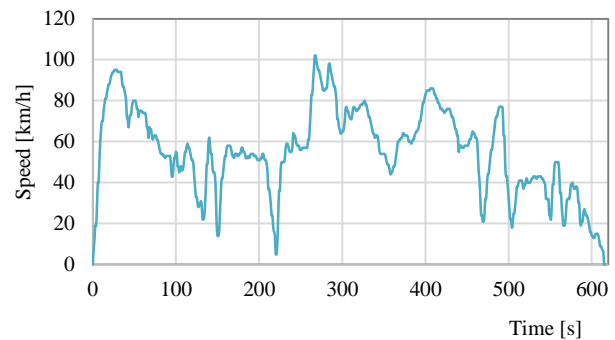


Fig. 3. Speed profile during the road tests

The HEV's speed varied from 0 km/h to 102 km/h over the entire period of time. The values of this parameter were characteristic for urban driving (less than or equal to 50 km/h) and extra-urban driving (greater than 50 km/h). When driving below 50 km/h, the electric drive mode of the HEV was frequently engaged. Above this speed, the electric hybrid powertrain was operating in the Normal Drive Mode (NORMAL)

## 4.3. Power of energetic machines

On Figure 4, the degree of electrochemical charge of the energy storage system is presented. It is worth noting that the applied model predictive control contributes to a higher level of charge of the traction battery while driving.

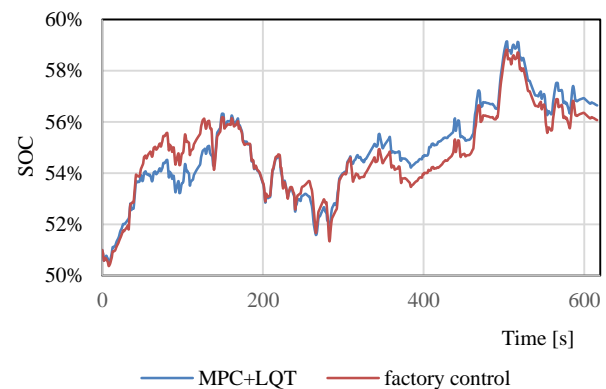


Fig. 4. Level of charge of the traction battery

This is due to the energy accumulation system power values (Fig. 5), which translate into the level of battery charge. Negative power indicates charging of the energy storage system, while positive power indicates the discharging thereof.

For the factory control, the power of the traction battery varies from -17.87 to 26.96 kW. For the model predictive control, the power of the traction battery varies from -20.16 to 27.85 kW.

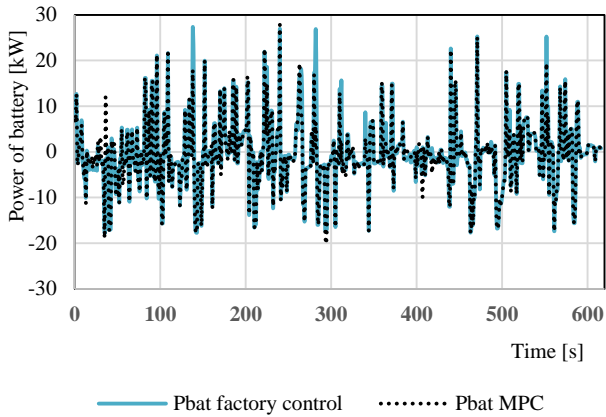


Fig. 5. Power of battery

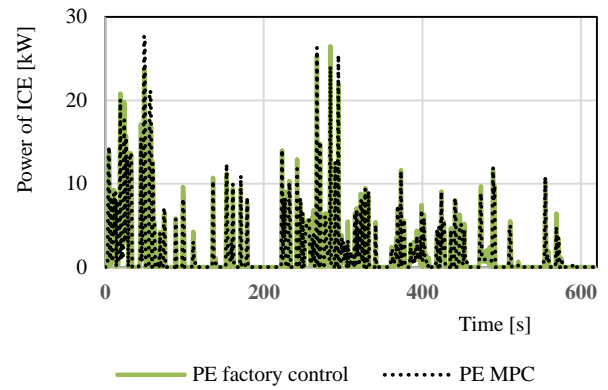


Fig. 7. Power of ICE

For the factory control, the power of the internal combustion engine varies from 0 to 26.50 kW. For the model predictive control, the power of the internal combustion engine varies from 0 to 27.58 kW. It can be concluded that the change of control type has an impact on the change of the power value of the internal combustion engine.

An important fact is that the power of the battery depends on the power balance of the generator and the electric motor. Hence, the negative power values of the electrochemical energy storage system indicate that the power is being recovered. This can be achieved during regenerative braking of the vehicle. Positive values of battery power indicate the use of energy accumulated in it.

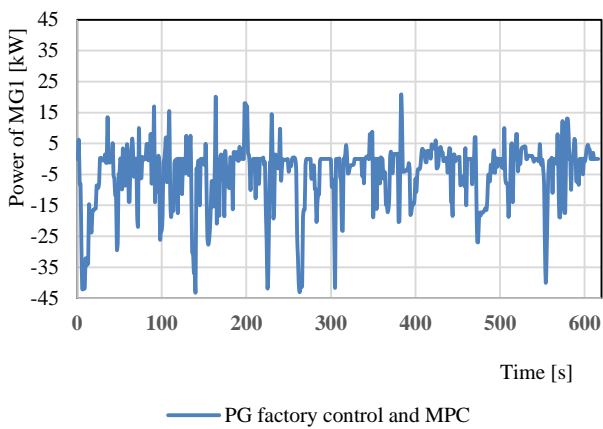


Fig. 6. Power of MG1

For the factory control and for model predictive control, the power of the MG1 varies from -43.09 to 20.49 kW.

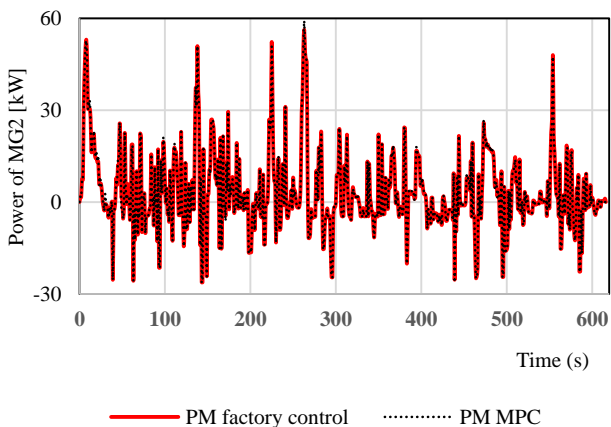


Fig. 6. Power of MG2

For the factory control, the power of the MG2 varies from -26.19 to 56.24 kW. For the predictive control, the power of the traction battery varies from -26.19 to 59.16 kW.

#### 4.4. Rotational velocities of energy machines

Rotational velocities of energetic machines (Fig. 8) are the same for both factory control and model predictive control of the system.

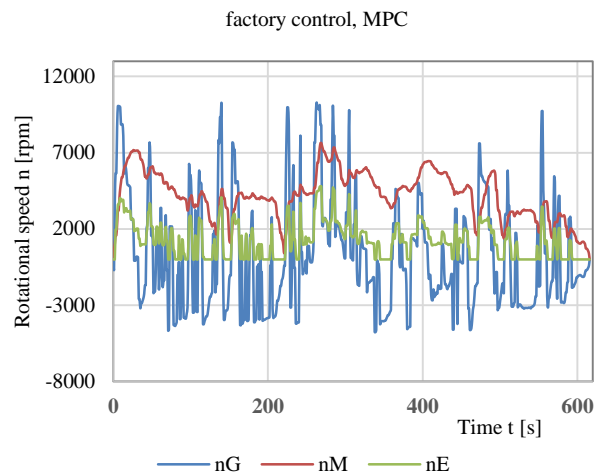


Fig. 8. Rotational speeds of energetic machines

The rotational speed of the internal combustion engine is between 0 and 4800 rpm. The rotational speed of the generator is between -4769 and 10,292 rpm. The rotational speed of the electric motor is between 0 and 7630 rpm.

### 4.5. Fuel consumption of internal combustion engine and electric motor

Figure 9 and Fig. 10 show the equivalent consumption of fuel of the battery and the fuel consumption of the internal combustion engine.

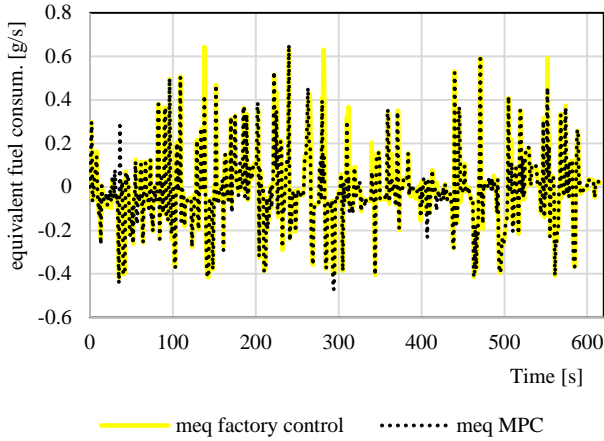


Fig. 9. Equivalent fuel consumption

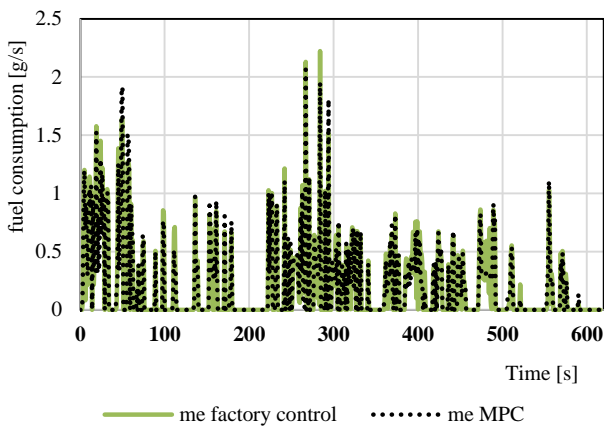


Fig. 10. Fuel consumption

In the course of the factory control mode, the equivalent fuel consumption is between  $-0.42$  g/s and  $0.63$  g/s. For model predictive control equivalent fuel consumption values range from  $-0.47$  g/s to  $0.65$  g/s.

The fuel consumption of the internal combustion engine reaches values from 0 to  $2.22$  g/s (factory control) and from 0 to  $2.06$  g/s (MPC).

### 4.6. Power map of the internal combustion engine

Figure 11 presents power maps of the internal combustion engine in the course of factory and model predictive control.

On the basis of the graphs, some differences can be noticed in the location of the useful power values of the engine (with factory control and model predictive control).

In the case of the factory control, the useful power values are distributed in the range from 0 to  $26.5$  kW. This corresponds to an overall engine efficiency from 0 to 34%. In the case of the model predictive control, most of the

useful power of the internal combustion engine is concentrated in the range from 0 to  $27.6$  kW. For this type of control, the overall efficiency values of the internal combustion engine are between 0 and 34%.

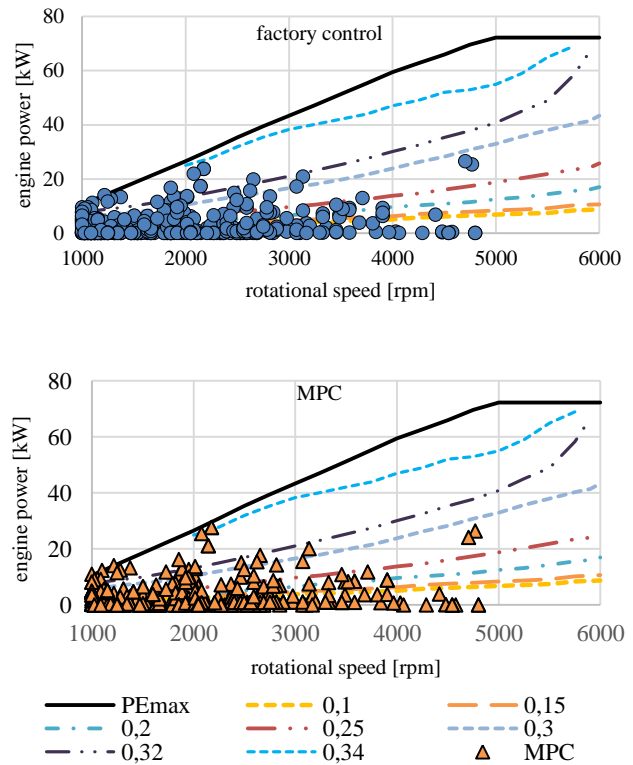


Fig. 11. Power map of the internal combustion engine

### 5. Model validation

Model validation was based on comparison of fuel consumption value of the HEV according to the manufacturer, factory control and MPC with LQT (Table 5).

Table 5. Mileage fuel consumption

	mileage fuel consumption	
	[dm <sup>3</sup> /100 km]	[mpg]
factory control	1.90	123.78
MPC	1.79	130.98
Manufacturer	2.10	111.87

The mileage consumption of the Toyota Prius 3 (2012) HEV provided by the manufacturer was determined on the basis of tests in established laboratory conditions (for a mixed cycle). It is 10% higher than the value of the mileage consumption of the HEV obtained on the presented route. The difference may be due to different measurement conditions. This could have been caused by other speed and acceleration values in road conditions, additional electric receivers turned off on the route, etc. The simulation of energy management of energetic machines according to MPC allowed to reduce the mileage fuel consumption from  $1.90$  to  $1.79$  dm<sup>3</sup>/100 km. This is the HEV fuel consumption savings of 4%.

## 6. Conclusion

The mileage consumption of the Toyota Prius 3 (2012) HEV provided by the manufacturer was 10% higher than the value of the mileage consumption of the HEV obtained on the presented route. The evaluation of the HEV mileage fuel consumption in real road conditions according to MPC with 13 reference trajectories showed total fuel savings of 4%. The energy management system used have good effect on SOC in comparison to factory control. Under MPC (with 13 reference trajectories) at the end of the course SOC was 6.7 % higher than under factory control. Changes of SOC – factory control: from 50.1% (the beginning) to 56.1% (the end of course); for MPC from 50.1% (the beginning) to 59.9% (the end of the course). The research method used was a case study. The values of the mileage fuel consumption were considered for one specific HEV model (and one

specific route). Due to the great similarity in the design of the drive system of the test object and other HEVs, it can be assumed that the test results were general in nature. The percentage improvement in fuel economy in MPC can also translates into other HEVs. The adopted work methodology contained certain limitations. They included, among others road tests in urban and extra-urban conditions (motorway conditions have not been taken into account) as well as considering only mileage fuel consumption. The directions of future research follow directly from the limitations. It would be worth carrying out road tests of HEV fuel consumption with MPC not only in urban and extra-urban conditions, but also in highway conditions. An interesting idea would also be road tests of HEV exhaust emissions with MPC.

## Nomenclature

HEV	hybrid electric vehicle	$P_{\text{resis}}$	resistance power (kW)
ICE	internal combustion engine	$Q_{\text{max}}$	maximum battery capacity (Ah)
MPC	model predictive control	$Q_{\text{used}}$	battery capacity used (Ah)
MG1	generator	$r_{\text{bat}}$	internal battery resistance ( $\Omega$ )
MG2	electric motor	$r_d$	dynamic wheel radius (m)
$A_f$	frontal area of vehicle ( $\text{m}^2$ )	$R$	number of teeth of the ring gear (m)
$b$	specific fuel consumption (kg/Ws)	$R_1$	number of crown wheel teeth (m)
$C_d$	air drag resistance coefficient	$R_2$	number of ring wheel teeth on the electric motor side (m)
$C_1$	number of teeth of the first set satellites (m)	$s$	step
$C_2$	number of teeth of the second set of satellites (m)	SOC	state of charge (%)
$f_d$	total gear ratio	$\text{SOC}_d$	desired state of charge (%)
$f_r$	rolling resistance coefficient	$S_1$	number of teeth of the first sun gear (m)
$F_a$	air resistance (N)	$S_2$	number of teeth of the second sun gear (m)
$F_i$	inertia resistance (N)	$t$	time (s)
$F_p$	propelling force (N)	$t_d$	jump (step level)
$F_r$	rolling resistance (N)	$T_{\text{brk}}$	brake torque (Nm)
$F_s$	slope resistance (N)	$T_{\text{des}}$	desired torque (Nm)
$F_1$	internal force between teeth of the first gear (N)	$U_{\text{bus}}$	voltage in the battery circuit (V)
$F_2$	internal force teeth force of the second gear (N)	$v_{\text{veh}}$	vehicle speed (m/s)
$\text{fuel}_s$	fuel consumption (g)	$V_{\text{OC}}$	open-circuit voltage of the battery (V)
$g$	gravitational acceleration ( $\text{m/s}^2$ )	$W_u$	calorific value of fuel (J/kg)
$I_{\text{bat}}$	battery charging/discharging current (A)	$\alpha$	slope of elevation ( $^\circ$ )
$J$	cost function (g)	$\alpha_E$	penalty factor
$J_E$	mass moment of inertia of the ICE ( $\text{kgm}^2$ )	$\omega_{C1}$	angular speed of the satellite yoke $C_1$ (1/s)
$J_G$	mass moment of inertia of the MG1 ( $\text{kgm}^2$ )	$\omega_E$	angular speed of the ICE (1/s)
$J_R$	mass moment of inertia of the planetary gear ring wheel ( $\text{kgm}^2$ )	$\omega_G$	angular speed of the generator (1/s)
$J_M$	mass moment of inertia of the MG2 ( $\text{kgm}^2$ )	$\omega_M$	angular speed of the electric motor (1/s)
$m$	total mass of vehicle (kg)	$\omega_R$	angular speed of the crown wheel R (ring) (1/s)
$\dot{m}$	actual fuel consumption (kg/s)	$\omega_{s1}$	angular speed of the sun wheel S1 (1/s)
$\dot{m}_{\text{eq}}$	equivalent fuel consumption (kg/s)	$\omega_{s2}$	angular speed of the sun wheel S2 (1/s)
$N$	number of steps	$\rho$	coefficient occurring between the tracking error and the equivalent fuel consumption
$P_{\text{bat}}$	power of battery (W)	$\rho_A$	air density ( $\text{kgm}^{-3}$ )
$P_E$	power of the ICE (kW)	$\eta_{\text{coulomb}}$	Coulomb efficiency
$P_G$	generator power (kW)	$\eta_{C1}$	generator efficiency
$P_M$	electric motor power (kW)	$\eta_{C2}$	motor efficiency
$P_R$	power of the ring gear of the planetary gear (kW)	$\eta_{C1/R}$	efficiency between the first set satellites and the ring gear
$P_{E\text{des}}$	desired power of the ICE (kW)	$\eta_E$	overall engine efficiency
$P_{G\text{des}}$	desired power of the generator (kW)	$\eta_{fd}$	final drive efficiency
$P_{M\text{des}}$	desired power of the electric motor (kW)		
$P_{\text{pre}}$	expected system power (kW)		

$\eta_{R2R}$	efficiency between the second ring wheel teeth and the ring gear	$\tau_E$	internal combustion engine operation time (s)
$\eta_{S1/C1}$	efficiency between the first sun gear and the first set of satellites	$\tau_G$	generator operation time (s)
		$\tau_M$	electric motor operation time (s)

## Bibliography

- [1] Abido MA. Optimal power flow using particle swarm optimization. *Int J Elec Power*. 2002;24:563-571. [https://doi.org/10.1016/S0142-0615\(01\)00067-9](https://doi.org/10.1016/S0142-0615(01)00067-9)
- [2] Back M. Prädiktive Antriebsregelung zum Energieoptimalen Betrieb von Hybridfahrzeugen. 2004. Dissertation, Univ. Karlsruhe.
- [3] Barsali S, Miulli C, Possenti A. A control strategy to minimize fuel consumption of series hybrid electric vehicles. *IEEE Trans Veh Technol*. 2004;19(1):187-195. <https://doi.org/10.1109/TEC.2003.821862>
- [4] Bieniek A, Graba M, Mamala J, Praznowski K, Hennek K. Energy consumption of a passenger car with a hybrid powertrain in real traffic conditions. *Combustion Engines*. 2022;191(4):15-22. <https://doi.org/10.19206/CE-142555>
- [5] Borhan HA, Vahidi A. Model predictive control of a power-split hybrid electric vehicle with combined battery and ultracapacitor energy storage. *Proceedings of the 2010 American Control Conference*. 2010:5031-5036. <https://doi.org/10.1109/ACC.2010.5530728>
- [6] Cao J, Peng J, He H. Modeling and simulation research on power-split hybrid electric vehicle. *Energy Proced*. 2016;104:354-359. <https://doi.org/10.1016/j.egypro.2016.12.060>
- [7] Chen S-Y, Hung Y-H, Wu C-H, Huang S-T. Optimal energy management of a hybrid electric powertrain system using improved particle swarm optimization. *Appl Energy*. 2015;160:132-145. <https://doi.org/10.1016/j.apenergy.2015.09.047>
- [8] Chen Z, Xiong R, Cao J. Particle swarm optimization-based optimal power management of plug-in hybrid electric vehicles considering uncertain driving conditions. *Energy*. 2016; (96):197-208. <https://doi.org/10.1016/j.energy.2015.12.071>
- [9] Chen Z, Xiong R, Wang K, Jiao B. Optimal energy management strategy of a plug-in hybrid electric vehicle based on a particle swarm optimization algorithm. *Energies*. 2015;8:3661-3678. <https://doi.org/10.3390/en8053661>
- [10] Delprat S, Lauber J, Guerra TM, Rimaux J. Control of a parallel hybrid powertrain: optimal control. *IEEE Trans Veh Technol*. 2004;53(3):872-881. <https://doi.org/10.1109/tvt.2004.827161>
- [11] Gao J, Zhu G, Strangas E, Sun F. Equivalent fuel consumption optimal control of a series hybrid electric vehicle. *P I Mech Eng D-J Aut*. 2009;23:1003-1018. <https://doi.org/10.1243/09544070JAUTO107>
- [12] Golebiewski W, Lisowski M. Theoretical analysis of electric vehicle energy consumption according to different driving cycles. *IOP Conf Ser Mater Sci Eng*. 2018;421:022010. <https://doi.org/10.1088/1757-899X/421/2/022010>
- [13] Grudzinski P. Toyota Hybrid Drive System. Toyota Motor Poland. 2022.
- [14] Guzzella L, Sciarretta A. Vehicle Propulsion Systems. Introduction to Modeling and Optimization. Berlin: Springer-Verlag. 2005, 190.
- [15] Hwang H-Y, Chen J-S. Optimized fuel economy control of power – split hybrid electric vehicle with particle swarm optimization. *Energies*. 2020;13:2278. <https://doi.org/10.3390/en13092278>
- [16] Kim TS, Manzie C, Sharma R. Model predictive control of velocity and torque split in a parallel hybrid vehicle. *IEEE Sys Man Cyber*. 2009:2014-2019.
- [17] Kleimaier A, Schroder D. An approach for the online optimized control of a hybrid powertrain. 7th International Workshop on Advanced Motion Control. 2002:215-220. <https://doi.org/10.1109/AMC.2002.1026919>
- [18] Lin CC, Peng H, Grizzle JW, Kang J-M. Power management strategy for a parallel hybrid electric truck. *IEEE T Contr Syst T*. 2003;11(6):839-849. <https://doi.org/10.1109/TCST.2003.815606>
- [19] Lin CC, Peng H, Grizzle JW. A stochastic control strategy for hybrid electric vehicles. *P Amer Contr Conf*. 2004; (5):4710-4715. <https://doi.org/10.23919/ACC.2004.1384056>
- [20] Liu J, Peng H. Modeling and control of a power-split hybrid vehicle. *IEEE T Contr Syst T*. 2008;16(6):1242-1251. <https://doi.org/10.1109/TCST.2008.919447>
- [21] Liu J, Peng H. Automated modelling of a power-split hybrid vehicles. *IFAC P Vol*. 2008;41(2):4648-4653. <https://doi.org/10.3182/20080706-5-KR-1001.00782>
- [22] Merksiz J, Pielecha I. Układy mechaniczne pojazdów hybrydowych. Wydawnictwo Politechniki Poznańskiej. Poznan 2015.
- [23] Moura SJ, Fathy HK, Callaway DS, Stein JL. A stochastic optimal control approach for power management in plug-in hybrid electric vehicles. *IEEE T Veh Technol*. 2011;19: 545-555. <https://doi.org/10.1109/TCST.2010.2043736>
- [24] Musado C, Rizzoni G, Guezennec Y, Staccia B. A ECMS: an adaptive algorithm for hybrid electric vehicle energy management. *Eur J Control*. 2005;11(4-5):509-524. <https://doi.org/10.3166/ejc.11.509-524>
- [25] Paganelli G, Delprat S, Guerra T, Rimaux J, Santin J. Equivalent consumption minimization strategy for parallel hybrid powertrains. *IEEE Vehicular Technology Conference*. 2002;4:2076-2081. <https://doi.org/10.1109/VTC.2002.1002989>
- [26] Paganelli G, Guezennec Y, Rizzoni G. Optimizing control strategy for hybrid fuel cell vehicle. *SAE Technical Paper* 2002-01-0102, 2002. <https://doi.org/10.4271/2002-01-0102>
- [27] Pielecha I, Cieślak W, Fluder K. Analysis of energy management strategies for hybrid electric vehicles in urban driving conditions. *Combustion Engines*. 2018;173(2):14-18. <https://doi.org/10.19206/CE-2018-203>
- [28] Prajwowski K, Golebiewski W, Lisowski M, Abramek KF, Galdynski D. Modeling of working machines synergy in the process of the hybrid electric vehicle acceleration. *Energies*. 2020;13:5818. <https://doi.org/10.3390/en13215818>
- [29] Prajwowski K, Golebiewski W, Lisowski M, Eliaz J. Road tests of selected electrical parameters of hybrid vehicle accumulation system. *IEEE Trans Veh Technol*. 2021;70(1): 203-211. <https://doi.org/10.1109/TVT.2020.3043852>
- [30] Sciarretta A, Back M, Guzzella L. Optimal control of parallel hybrid electric vehicles. *IEEE T Contr Syst T*. 2004; 12(3):352-363. <https://doi.org/10.1109/TCST.2004.824312>
- [31] Shi DH, Wang SH, Pisu P, Chen L, Wang RC, Wang RG. Modeling and optimal energy management of a power split hybrid electric vehicle. *Sci China Technol Sc*. 2017;60:713-725. <https://doi.org/10.1007/s11431-016-0452-8>

- [32] Tang X, Chen J, Liu T, Qin Y, Cao D. Distributed deep reinforcement learning- based energy and emission management strategy for hybrid electric vehicles. *IEEE T Veh Technol.* 2021;70(10):9922-9934. <https://doi.org/10.1109/TVT.2021.3107734>
- [33] Wu X, Cao B, Wen J, Bian Y. Particle swarm optimization for plug-in hybrid electric vehicle control strategy parameter. *2008 IEEE Vehicle Power.* 2008:1-5. <https://doi.org/10.1109/VPPC.2008.4677635>
- [34] Yang J, Zhu G. Adaptive recursive prediction of the desired torque of hybrid powertrain. *IEEE T Veh Technol.* 2015; 64(8):3402-3413. <https://doi.org/10.1109/tvt.2014.2357395>
- [35] Yang J, Zhu G. Model predictive control of a power split hybrid powertrain. *Amer Contr Conf.* 2016:617-622. <https://doi.org/10.1109/ACC.2016.7524982>
- [36] Yu K, Yang J, Yamaguchi D. Model predictive control for hybrid vehicle ecological driving using traffic signal and road slope information. *Control Theory Technol.* 2015; 13(1):17-28. <https://doi.org/10.1007/s11768-015-4058-x>
- [37] Zhu Y, Chen Y, Tian G, Wu H, Chen Q. A four-step method to design an energy management strategy for hybrid vehicles. *P Amer Contr Conf.* 2004;1:156-161. <https://doi.org/10.23919/ACC.2004.1383596>
- [38] Zhu D, Pritchard E, Dadam SR, Kumar V, Xu Y. Optimization of rule-based energy management strategies for hybrid vehicles using dynamic programming. *Combustion Engines.* 2021;184(1):3-10. <https://doi.org/10.19206/CE-131967>

Wawrzyniec Gołębiewski, DEng. – Faculty of Mechanical Engineering, West Pomeranian University of Technology in Szczecin, Poland.  
e-mail: [wawrzyniec.golebiewski@zut.edu.pl](mailto:wawrzyniec.golebiewski@zut.edu.pl)



Prof. Krzysztof Danilecki, DSc., DEng. – Faculty of Mechanical Engineering, West Pomeranian University of Technology in Szczecin, Poland.  
e-mail: [krzysztof.danilecki@zut.edu.pl](mailto:krzysztof.danilecki@zut.edu.pl)



Konrad Prajwowski, DEng. – Faculty of Mechanical Engineering, West Pomeranian University of Technology in Szczecin, Poland.  
e-mail: [konrad.prajwowski@zut.edu.pl](mailto:konrad.prajwowski@zut.edu.pl)



Mirosław Radwan, MSc., Lieutenant Colonel – Command of Territorial Defense Forces, Poland.  
e-mail: [mirek\\_swir@poczta.onet.pl](mailto:mirek_swir@poczta.onet.pl)



Prof. Maciej Lisowski, DSc., DEng. – Faculty of Mechanical Engineering, West Pomeranian University of Technology in Szczecin, Poland.  
e-mail: [maciej.lisowski@zut.edu.pl](mailto:maciej.lisowski@zut.edu.pl)

